

Strain Rate Behavior of Closed-Cell Al-Si-Ti Foams: Experiment and Numerical Modeling

Jian Zhang, Gui-Ping Zhao, Tian-Jian Lu & Si-Yuan He

To cite this article: Jian Zhang, Gui-Ping Zhao, Tian-Jian Lu & Si-Yuan He (2015) Strain Rate Behavior of Closed-Cell Al-Si-Ti Foams: Experiment and Numerical Modeling, *Mechanics of Advanced Materials and Structures*, 22:7, 556-563, DOI: [10.1080/15376494.2013.828813](https://doi.org/10.1080/15376494.2013.828813)

To link to this article: <http://dx.doi.org/10.1080/15376494.2013.828813>



Accepted author version posted online: 04 Feb 2015.
Published online: 04 Feb 2015.



Submit your article to this journal [↗](#)



Article views: 106



View related articles [↗](#)



View Crossmark data [↗](#)



Citing articles: 2 View citing articles [↗](#)

Strain Rate Behavior of Closed-Cell Al-Si-Ti Foams: Experiment and Numerical Modeling

JIAN ZHANG¹, GUI-PING ZHAO¹, TIAN-JIAN LU¹, and SI-YUAN HE²

¹State Key Laboratory for Mechanical Structure Strength and Vibration, School of Aerospace, Xi'an Jiaotong University, Xi'an, China

²Department of Materials Science and Engineering, Southeast University, Nanjing, China

Received 5 April 2012; accepted 4 February 2013.

We present a combined experimental and numerical study on the strain rate effect of closed-cell Al-Si-Ti foams having different relative densities fabricated using the powder metallurgy foaming technique. The high strain rate tests were conducted with split Hopkinson pressure bar technique at 800 to 2500 s⁻¹. Two-dimensional mesoscale finite element models were created from tomographic images of the homologous foam. The rate sensitivity of the foam originates mainly from that of its parent material, increasing with increasing relative density. Stress elevation due to other effects, such as micro-inertia, shock wave, and gas pressure in individual cells, is negligible.

Keywords: metallic foams, powder metallurgy, split Hopkinson pressure bar, pulse shaper, mesoscale finite element model, dynamic compression

1. Introduction

High porosity cellular metallic foams have been considered as a candidate energy dissipation material under dynamic loading conditions due to their large deformation capability at nearly constant plateau stress [1]. A proper understanding of their compressive behavior at high strain rates, especially the strain rate effect on the plateau stress is therefore important. To measure the dynamic mechanical properties of aluminum foams at high strain rates, the split Hopkinson pressure bar (SHPB) technique has been widely employed. Existing SHPB test results summarized in Table 1 show conflicting results for the rate sensitivity of closed-cell aluminum foams. For instance, at the same relative density, aluminum foams (IFAM) produced using the powder metallurgy technique exhibit discrepant strain rate sensitivities [2–4]. To date, the strain rate sensitivity of metallic foams is not fully clear because various types of foam made from different manufacturing processes exist. The issue is complicated further by the dependence of the rate sensitivity upon foam relative density, micro-inertia, cell-wall material, specimen size, etc.

In the present study, to investigate the strain rate sensitivity behavior of aluminum foams, closed-cell Al-Si-Ti foams with

different relative densities were first produced using the powder metallurgy foaming technique. Quasi-static compressive tests as well as high strain rate SHPB tests were subsequently carried out. Based upon the tomographic images of the Al-Si-Ti foam, finite element (FE) simulations were carried out. The influence of foam relative density, cell-wall material, micro-inertia, shock wave and gas pressure on foam rate sensitivity was systematically studied. The effect of specimen size was also brought forward to explain the difference of compressive stress versus strain curves obtained from quasi-static uniaxial compression and SHPB tests.

2. Material and Testing

Closed-cell Al-Si-Ti foams were produced using powder metallurgy foaming technique with blowing agents. The composition of the cell-wall material is Al-7Si (by mass%) and titanium hydride (TiH₂, typically 1.0%), the latter serving as the blowing agent. The fabrication process is similar to that of closed-cell IFAM and Alulight foams. First, aluminum, silicon, and TiH₂ powders were blended evenly in proportion. The powder mixture was then cold compacted (at a pressure of 4.0 MPa) and hot extruded (to a ratio of 20:1 and at the temperature of 430°C) axially in a cylindrical chamber to obtain foamable precursor billet (diameter 45 mm and height 7.5 mm), with a relative density (density of foam block divided by that of cell-wall material, ρ/ρ_{solid}) more than 98%. During heat treatment inside a muffle furnace, the melt starts to expand slowly at about 640°C, eventually filling the cylindrical steel

Address correspondence to Gui-Ping Zhao, State Key Laboratory for Mechanical Structure Strength and Vibration, School of Aerospace, Xi'an Jiaotong University, No. 28, Xianning West Road, Xi'an 710049, China. E-mail: zhaogp@mail.xjtu.edu.cn
Color versions of one or more of the figures in the article can be found online at www.tandfonline.com/umcm.

Table 1. Strain rate effect of closed-cell aluminum foams

Foam type	Processing method	Material make	Relative density	Test method (SHPB)	Rate effect	References
IFAM	Powder metallurgy	Al-Ti	0.12–0.30	—	Insensitive	[2]
IFAM	Powder metallurgy	Al-Si-Ti	0.133, 0.211	—	Insensitive	[3]
IFAM	Powder metallurgy	Al-Si-Ti	0.23	Nylon bar	Sensitive	[4]
Alporas	Batch casting	Al-Ca-Ti-Fe-Mg	0.09–0.1	Steel bar	Sensitive	[5]
Alporas	Batch casting	Al-Ca-Ti	0.074–0.15	Aluminum bar	Sensitive	[6]
Alporas	Batch casting	Al-Ca-Ti	0.106–0.155	Magnesium alloy bar	Sensitive	[7]
Alporas	Batch casting	Al-Ca-Ti-Fe-Mg	0.08	Magnesium alloy bar	Sensitive	[8]
Cymat	Melt gas injection	Al-SiC	0.093	Nylon bar	Insensitive	[9]
Alulight	Powder metallurgy	Al-Si-Ti	0.17–0.40	Steel bar	Insensitive	[10]
—	Powder metallurgy	Al-Ti	0.062–0.373	Hollow aluminum bar	Sensitive	[11]
SiCp/AlSi9Mg	Powder metallurgy	Al-Si-Mg	0.21, 0.32	Aluminum alloy bar	Sensitive	[12]
Cenospheres	Squeeze casting	Pure Al	0.593, 0.563	Aluminum alloy bar	Sensitive	[13]
Composite foam	Powder metallurgy	Al-Mg-Ti-C _f	0.10–0.20	Steel bar	Sensitive	[14]

foaming vessel. Finally, upon cooling the vessel rapidly below the melting point of the alloy, the liquid foam turned into solid closed-cell Al-Si-Ti foam. Approximately homogeneous foams with different relative densities were obtained through careful adjustment of processing parameters, such as the amount of TiH₂ added and the heat treatment time after adding TiH₂, as shown in Figure 1.

For both quasi-static and dynamic compressive tests, cylindrical foam specimens with a diameter of 35 mm and a height of 10 mm were selected. To obtain reliable data of the aluminum foams, while the specimen diameter should be as large as possible within the limitations of the Hopkinson pressure bar (diameter of 37 mm), the specimen height should be as small as possible to avoid serious attenuation of stress waves traveling through the specimen. The choice of the present specimen dimensions insured each specimen had at least five cells along the height direction [15]. Photographs of foam

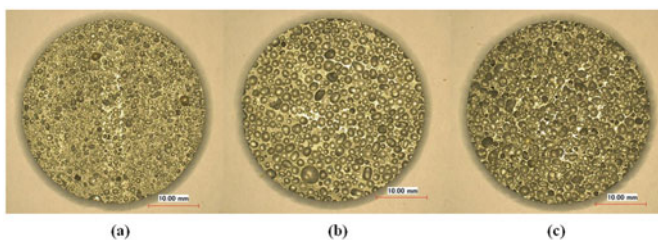


Fig. 1. Photograph of closed-cell Al-Si-Ti foam with relative density of: (a) 0.40, (b) 0.30, and (c) 0.21.

specimens with relative densities 0.40, 0.30, and 0.21 are shown in Figure 1, with average cell sizes measured as 0.9, 1.6, and 2.2 mm, respectively. To minimize damage to cell edges, the specimens were cut from the cast foam block with an electro-discharge machine (EDM).

Quasi-static compressive tests were performed on a displacement controlled servo-hydraulic test machine (MTS858 Minibionix, MTS Corporation, USA). Axial displacement was recorded to determine the nominal strain of the foam specimen while engineering stress was measured by load cell mounted on the testing machine. The tests were conducted at a cross-head speed of 0.01 mm/s, corresponding to a nominal strain rate of 0.001 s⁻¹.

High strain rate tests were performed using a SHPB apparatus (see Figure 2) within the strain rate range of 800 to 2500 s⁻¹. The apparatus comprises a 37-mm diameter striker, incident, transmitter, and absorbed bars, which are 600, 2000, 2000, and 800 mm in length, respectively, and all the bars were made of aluminum alloy. The foam specimen was sandwiched between the incident and transmitter bars, and a thin Vaseline layer was evenly spread on the loading surfaces to minimize friction effects. A small circular shaper (sheet) was placed on the impact face of the incident bar (see Figure 2) to produce slowly rising incident pulse and minimize wave dispersion effects, generating a constant strain rate in the plastic response regime [16]. Typically, the shaper materials are paper, aluminum, copper, brass, and stainless steel. However, after repeated attempts, 1.0- to 2.0-mm-thick lead sheets were selected as the ductile, very soft, highly malleable lead sheet caused no damage to the striker as well as the incident bar.

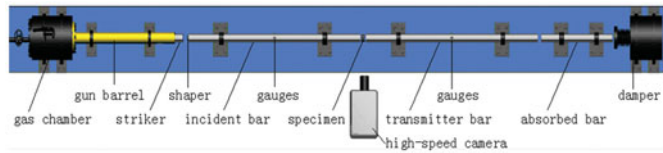


Fig. 2. SHPB set-up.

As shown in Figure 3, the shaped incident wave is relatively smooth while the reflected wave has a nearly constant platform, implying that the specimen deforms at a constant strain rate over most of the impact duration. Electrical resistance strain gauges attached to the middle surface of the incident bar were used to record both incident and reflected waves. Due to impedance mismatch between the specimen (Al-Si-Ti foam) and pressure bar (aluminum alloy), the transmitted signal is, in general, rather weak. Common approaches for raising the signal-to-noise level of the transmitted wave are: (1) low impedance material for transmitter bar, e.g., PMMA [10], magnesium alloy [7], and nylon [9]; (2) hollow aluminum transmitter bar [11]; (3) highly sensitive strain gauges [17]. In the present study, for simplicity highly sensitive semiconductor strain gauges were selected, which were glued to the transmitter bar surface. Since the sensitivity of semiconductor strain gauges is about 50 times higher than that of traditional electrical resistance strain gauges, the weak transmitted wave could be properly recorded, as demonstrated in Figure 3. The test results were analyzed based on the propagation principles of the longitudinal elastic wave in cylindrical bars, with the strain rate $\dot{\epsilon}(t)$, strain $\epsilon(t)$, and stress $\sigma(t)$ in the foam specimen calculated using the two-waves method [18].

3. Two-Dimensional Finite Element Models

Two-dimensional (2D) mesoscale FE models were created from tomographic images of closed-cell Al-Si-Ti foams,

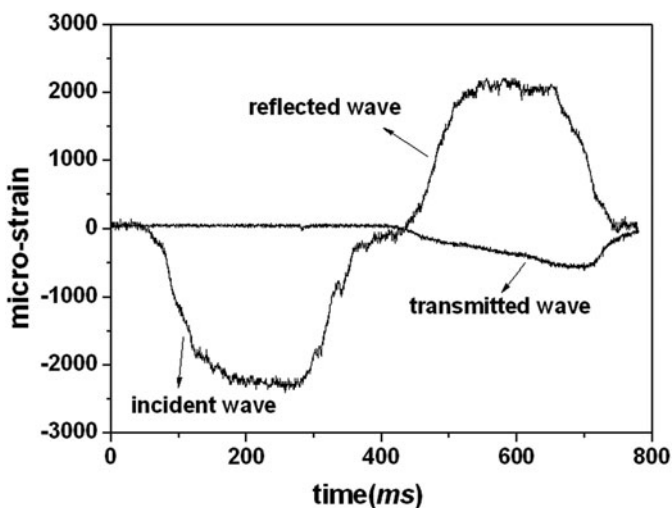


Fig. 3. Typical waveforms (including incident, reflected, and transmitted waves) from SHPB test.

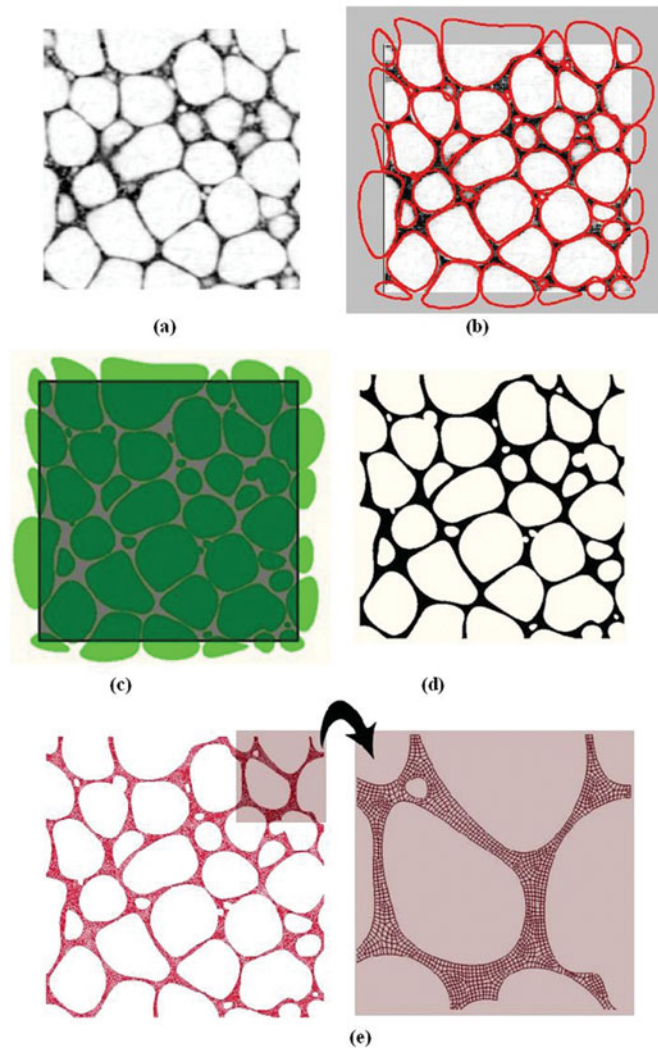


Fig. 4. Procedures for creating 2D mesoscale FE foam model with relative density of 0.2: (a) 2D tomographic image of aluminum foam; (b) cell-representing closed splines; (c) cell-representing regions; (d) 2D geometric model of aluminum foam; and (e) meshing with solid finite elements.

inspired by the methods of modeling 2D random Voronoi honeycombs [19] and X-ray tomography models [20]. As illustrated in Figure 4, the 2D mesoscale FE model for the case of relative density 0.2 was produced using the following procedures:

1. Acquire a typical 2D tomographic image of closed-cell Al-Si-Ti foam, Figure 4a;
2. Based on this image, draw closed splines to represent separated and smoothed cells, Figure 4b;
3. Change the closed splines into regions (marked as "A") and construct a square region (marked as "B") to represent the 2D specimen, Figure 4c;
4. Make a Boolean operation ("B" subtracting "A") to generate a 2D geometric cellular model, Figure 4d;

5. Extrude the 2D cellular model with a small thickness, and mesh the cellular model using solid elements, Figure 4e.

The present approach ensured the foam specimen models with relative densities of 0.2, 0.3, and 0.4 representing faithfully the irregular cell shape and unequally geometric distribution of the homologous foam.

The in-plane geometrical dimensions of the 2D FE foam model were taken as 10 mm × 10 mm, and its thickness was 0.02 mm (one element). To simplify the modeling, relatively small inner voids (less than 0.2 mm in diameter) were disregarded. Meshing with 8-node solid elements was achieved using the commercially available FE code ANSYS. The average element size was reduced to 0.04 mm to ensure numerical convergence. Mesh sensitivity studies revealed that further refinements did not appreciably improve the accuracy. The explicit finite element code LS-DYDA was employed to carry out all of the simulations.

The mechanical properties of the aluminum alloy (cell-wall material) were described using the isotropic hardening plastic material model within the LS-DYNA material library, with its density, Young's modulus, Poisson ratio, yield stress, and tangent modulus assigned as 2700 kg/m³, 69 GPa, 0.3, 76 MPa, and 0.69 GPa, respectively [21]. The strain rate effect of the aluminum alloy was accounted for by adding the Cowper–Symonds term to the constitutive relation [22]. If this term was removed, the strain rate effect of the cell-wall material was ignored.

To simulate numerically the boundary conditions applied in the present quasi-static and dynamic uniaxial compression tests, the FE foam model was sandwiched between two rigid plates. While the top plate was moving downward with a constant velocity, the bottom plate was kept stationary to ensure that the foam model deformed at constant strain rate; the foam model was confined along its out-of-plane direction while its two side edges were set free. It was further assumed that the top and bottom surfaces of the foam model can slip on both the rigid plates with a small friction coefficient (0.01) to represent the perfect lubricating condition in experiments. A sensitivity study was carried out and it was found that the simulation results were insensitive to the value chosen for the friction coefficient. For large deformation of the aluminum foam, automatic single surface contact options were applied to enforce hard contact between all potential cell-wall surfaces.

The 2D mesoscale FE model, as presented in Figure 4, can be conveniently used to represent the irregular cell shape and unequal geometric distribution of real foams. However, one limitation of the 2D model is that the discretization must be fine enough to properly model continuum cellular wall structures, i.e., the size of the elements must be sufficiently small. While 3D mesoscale FE models have also been used to simulate cellular foams, they are typically inefficient in terms of computation cost and, hence, rarely used in practical computation. Further, a 3D model constructed by using the present method would need hard work to repair the numerous process-induced geometrical defects present at the microscopic level. The 2D foam models were used in the present investigation to numerically simulate the mechanical behavior of model aluminum foams subjected to dynamic loading and quantify

the influence of key parameters, such as foam relative density, micro-inertia, cell-wall material, and specimen size, which may shed light on the underlying deformation mechanisms and cause for rate sensitivity of real aluminum foams. The simulation results are not directly used to compare with experimental measurement results.

4. Results and Discussion

4.1. Experimental Results

Figures 5a, 5b, and 5c present the uniaxial compressive stress versus strain curves obtained under three different strain rates for three relative foam densities, 0.40, 0.30, and 0.21. The results showed that, under either quasi-static or dynamic compression, the closed-cell Al-Si-Ti foams employed for the present study exhibited three distinctive deformation regions typical for cellular metals: initial elastic response, extended plateau region, and densification.

Here, to define whether the aluminum foam is sensitive or insensitive to strain rate, we adopted the criterion of 20% elevation in plateau stress [10]. For high relative density foams (e.g., 0.40), with the strain rate increasing from 0.001 to 2200 s⁻¹, the plateau stress was increased by about 40%, from 22.5 to 31.8 MPa. For foams with intermediate relative density ($\rho/\rho_{solid} = 0.30$), the plateau stress at 1800 s⁻¹ strain rate was about 25% higher than that at 0.001 s⁻¹. In comparison, no significant change in plateau stress was observed for low relative foam density (0.21) within the strain rate range of 0.001 to 2500 s⁻¹, consistent with existing findings for metallic foams having relatively low relative densities [2, 3]. For the present Al-Si-Ti foams with closed cells, a critical relative density (approximately 0.25) appeared to exist, above which the foam is strain rate sensitive. However, it must be emphasized that the critical value presented here should be used cautiously, as only three foam relative densities have been examined in the experiments and it is not yet clear whether this critical value is applicable to foams fabricated with other parent materials.

In general terms, the rate sensitivity of cellular metals may be affected by micro-inertia [9, 23–25]; rate sensitivity of cell-wall material [24, 26, 27]; compression of entrapped gas in cells [6, 11]; and other factors, such as inertia and shock wave effects [28] that may change the deformation mode of the material. Su et al. [22] suggested that, given the “flat topped” quasi-static stress versus strain curve of aluminum foams, micro-inertia plays little role under dynamic loading [10]. Therefore, in the following, the remaining factors that may cause the strain rate sensitivity of aluminum foams were discussed using the present FE simulation results.

4.2. Effect of Cell-Wall Material

Simulation results with FE models were analyzed for aluminum foams under different strain rates to investigate the rate effect of cell-wall material. Figure 6 presents the numerical results for selected foam relative densities. It was seen from Figure 6a that, when the cell-wall material was taken as rate sensitive, the simulated results followed the same trend

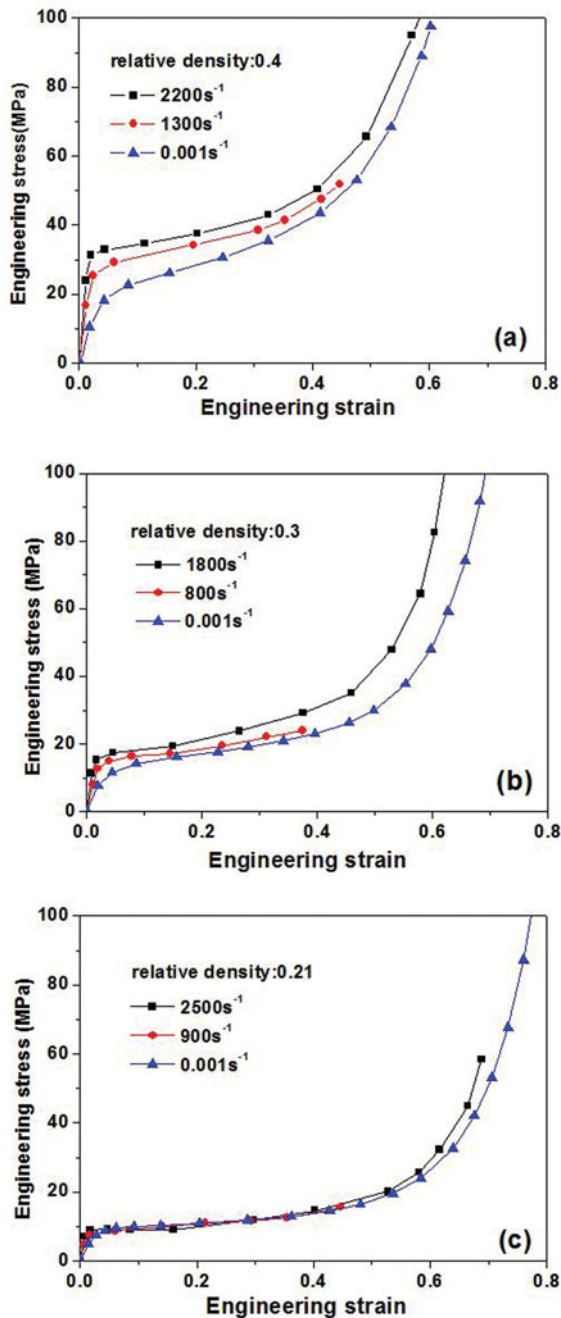


Fig. 5. Uniaxial compressive stress vs. strain curves experimentally measured at selected strain rates for closed-cell Al-Si-Ti foams with varying relative density: (a) 0.40, (b) 0.30, and (c) 0.21.

as that observed experimentally, i.e., Figure 5. However, if the rate dependence of the cell-wall material was neglected in the simulations, i.e., the Cowper–Symonds term was removed, the foams with varying relative densities did not exhibit significant dependence on strain rate. It appeared therefore that the strain rate sensitivity of the present aluminum foam may originate mainly from the strain rate sensitivity of its cell-wall material.

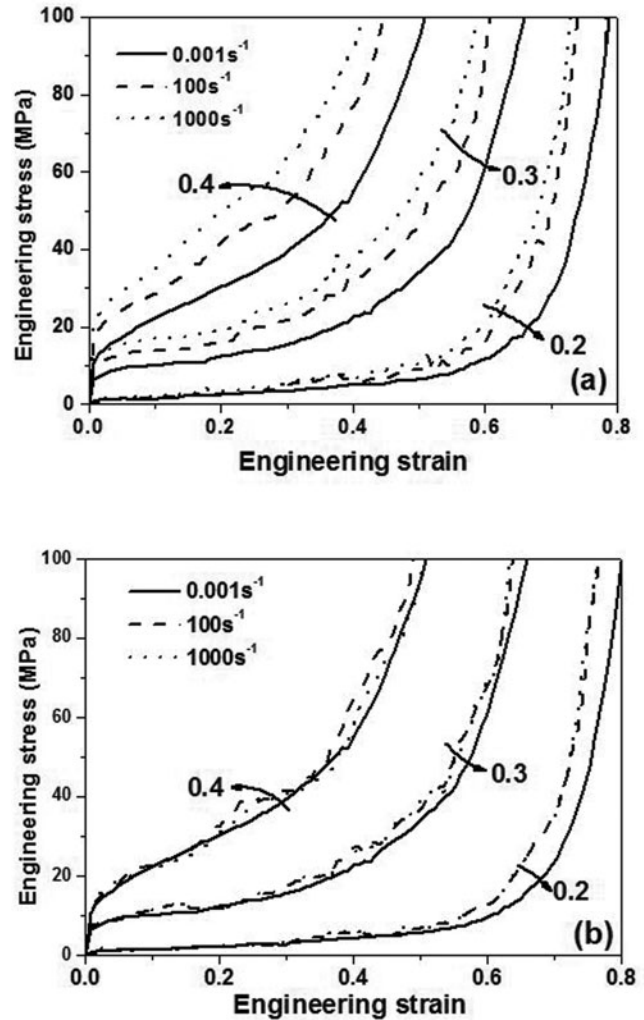


Fig. 6. Simulated uniaxial compressive stress vs. strain curves of aluminum foams made with (a) rate sensitive and (b) rate insensitive cell-wall material.

With foam relative density fixed, the deformation mode of the aluminum foam remained unchanged when the strain rate was increased from 0.001 to 1000 s^{-1} , as illustrated in Figure 7. For the three relative densities examined, it can be seen from Figure 7 that the deformation was first localized in the weakest region of the model specimen. For relatively high relative densities (e.g., 0.3 and 0.4), the deformation of the foam was dictated mainly by the narrowing of weak cells and the plastic flow of cell-wall material. As discussed in the previous section, at relatively high relative densities, the strain rate sensitivity of aluminum foams was derived mainly from that of the parent material. In contrast, when the relative density was reduced to 0.2, the foam deformation was mainly dominated by cell-wall buckling, as shown in Figure 7c. Here, the performance potential of the cell-wall material was not effectively developed and the dynamic compressive behavior of the foam was dependent mainly upon the shape and distribution of the cells, with the rate sensitivity of the cell-wall material playing a minor role.

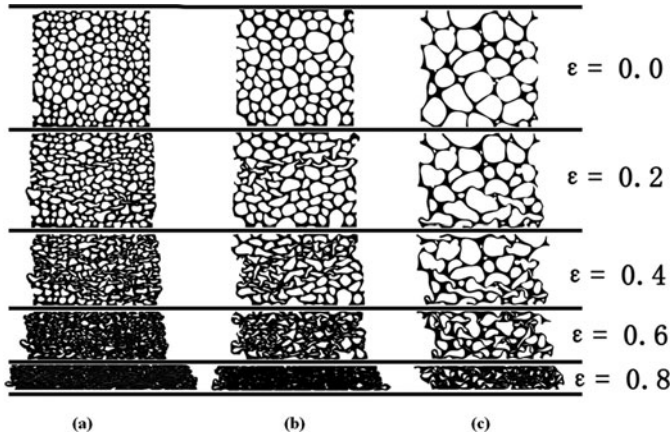


Fig. 7. Numerical deformation maps of the aluminum foams with relative densities: (a) 0.4, (b) 0.3, and (c) 0.2.

In summary, closed-cell aluminum foams fabricated from a rate-sensitive parent material can also exhibit strain rate sensitivity, which increases with the increase of foam relative density. However, while the numerically predicted critical sensitivity (~ 0.2) separating rate-sensitive and rate-insensitive regimes matches that experimentally observed (~ 0.25), this value is yet universally applicable as more experimental and numerical simulations concerning other cellular foams made from matrices having different rate dependent properties from the material system studied in this work.

4.3. Effect of Compressed Gas

To investigate the effects of compressed gas entrapped within the cells under dynamic compression, finite element simulations with a FE foam model (0.3) filled with gas medium (Figure 8) were carried out. The gas medium was filled by using the Lagrange method, same as the cell-wall material. The Null material and the Gruneisen equation of state were used to describe the mechanical behavior of the gas medium. When the change of gas volume reaches 0.5, the gas would discharge;

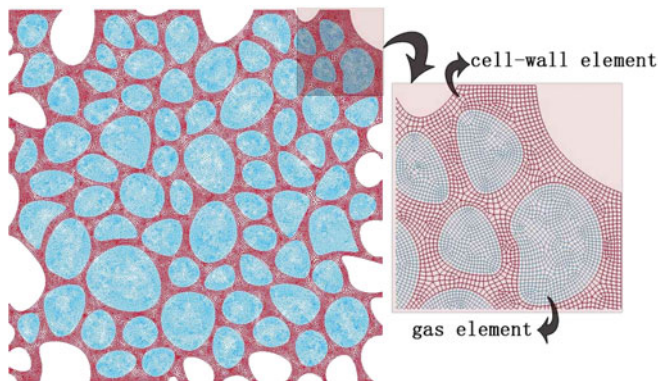


Fig. 8. Finite element model of aluminum foam filled with gas ($\rho/\rho_{solid} = 0.30$).

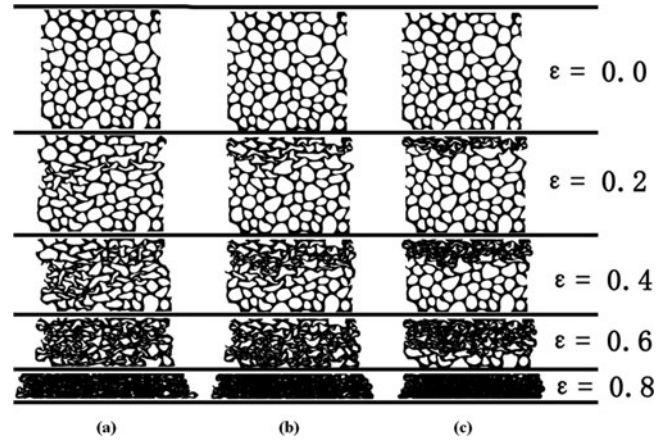


Fig. 9. Deformation mode of aluminum foams ($\rho/\rho_{solid} = 0.30$) with impact velocity: (a) 0.01 m/s, (b) 200 m/s, and (c) 400 m/s.

the corresponding elements were removed to avoid exceeding distortion of the element.

The simulation results (not presented here for brevity) demonstrated that, except for consuming more computing time, the presence of the gas medium did not change the dynamic strain-stress behavior of the aluminum foam, which is consistent with the finding of Gibson and Ashby [29] who calculated the contribution of compressed gas to the quasi-static strength of closed-cell foams. Also, according to Deshpande and Fleck [10], the stress elevation of the foam ($\rho/\rho_{solid} = 0.05$) due to compressed gas was no more than 0.05 MPa (less than 1.5%). Due to significant stiffness difference between the gas medium and the cell-wall material, the former can hardly affect the deformation of the latter. Consequently, the pressure due to compressed gas in the cells is too small to have any contribution to both the quasi-static and dynamic stress elevation of metal-based cellular materials [9, 10].

4.4. Effect of Inertia

When the impact velocity reaches the plastic wave velocity of aluminum alloy foams, the inertia (rather than micro-inertia) effect of the cell-wall material becomes important, with the deformation pattern of the foam changing from “random mode” to “shock mode” [30]. As shown in Figures 9b and 9c, the localized crushing band initiated at the impact end propagated like dominoes along the impact direction, significantly different from that of Figure 9a obtained under quasi-static loading. Further, the foam deformation was more localized as the impact velocity was increased.

The plastic wave velocity may be calculated as $C_p = \sqrt{E_p/\rho_s}$, where E_p and ρ_s are the plastic modulus and density of the cell-wall material, respectively. If the aluminum material has a “bi-linear” stress versus strain relation, with $E_p = 0.69$ GPa and $\rho_s = 2700$ kg/m³, then $C_p \approx 160$ m/s. (Note that the plastic wave velocity of a metallic foam is slightly smaller than that of its cell-wall material.) In the present SHPB tests, the largest compressive velocity reached was no more than 20 m/s, and hence the stresses at both the impact side and the

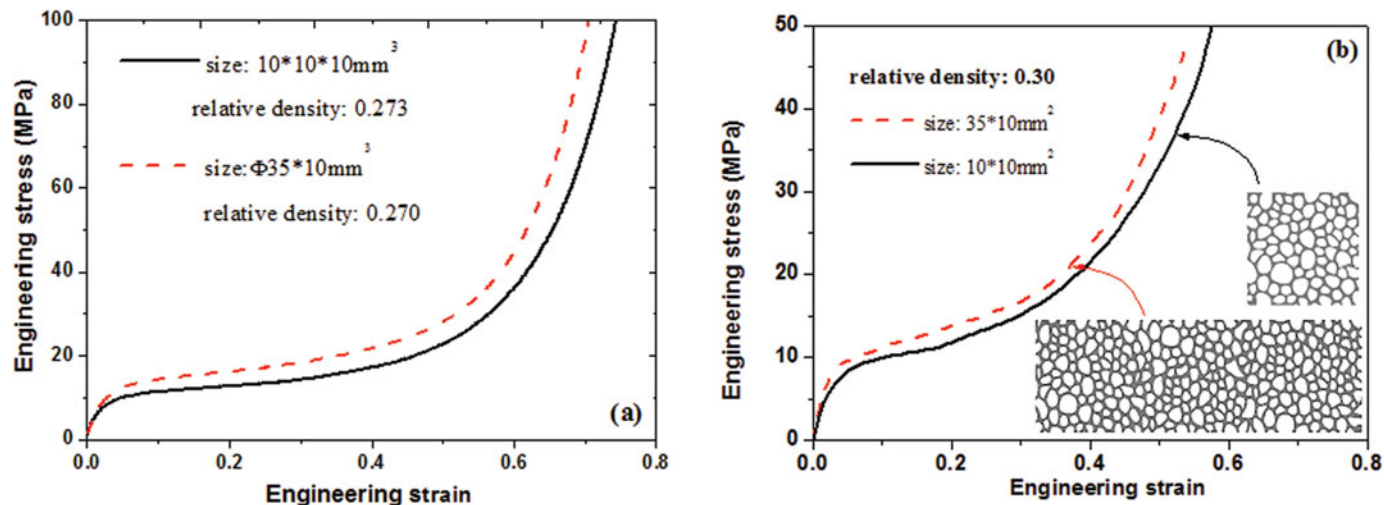


Fig. 10. Influence of specimen size on quasi-static stress vs. strain curve of closed-cell Al-Si-Ti foam: (a) measurement and (b) FE simulation.

stationary side of the foam specimen were uniform, with no “shock mode” deformation observed.

The strain rate effect and impact velocity are two different issues concerning the mechanical properties of closed-cell aluminum foams. When the impact velocity is low (less than the plastic wave velocity), the stress distributes uniformly in the foam so that the discussion of strain rate effect is relevant. When the impact velocity is sufficiently high, the foam deformation is dominated by “shock mode,” and the stresses at the impact side are significantly different from those at the stationary side. Under such conditions, the strain rate effect is overwhelmed by the inertia effect of the foam structure.

4.5. Effect of Specimen Size

Most existing studies on strain rate sensitivity of aluminum foams ignored the effect of specimen size. Actually, due to different test methods, the selected specimen sizes were usually different between dynamic and quasi-static compression tests [11–13, 17, 31–34]. For SHPB tests to obtain complete stress versus strain curves including the three distinctive regimes (linear elasticity, collapse plateau, and densification), the specimen height was commonly minimized [17, 34]. The slenderness ratio of foam specimens for MTS tests was therefore usually larger than that for SHPB tests.

Hanssen *et al.* [35] compared the quasi-static compressive strain versus stress curve of a cubic aluminum foam specimen and that with its height halved. They found that the latter exhibited about 15% enhancement of the initial plateau stress and far more strain hardening than the former, as shear failure occurring on the side wall of the cubic specimen led to reduced effective cross-sectional area.

To explore further the influence of specimen size (and shape), quasi-static compressive tests (strain rate fixed at 0.001 s^{-1}) were carried out on an MTS machine for the present Al-Si-Ti foams. The specimens selected were cube ($10 \times 10 \times 10 \text{ mm}^3$) and cylinder ($\text{Ø}35 \times 10 \text{ mm}^3$), respectively, while the foam relative density was fixed at 0.27. For the cylinder speci-

men, a new 2D mesoscale FE foam model (size $35 \times 10 \text{ mm}^2$, relative density 0.3) was constructed from a tomographic image of the homologous foam. The boundary conditions, cell-wall material properties, loading method, etc. remained unchanged as those employed in the previous model (size $10 \times 10 \text{ mm}^2$, relative density 0.3). From the obtained stress versus strain curves shown in Figure 10, it was found that both the experimental and numerical results exhibited consistent specimen size effect, and that specimen size had a relatively small influence on foam compression behavior, at least for the size range considered in the current study.

5. Concluding Remarks

A combined experimental and numerical simulation study was carried out to investigate the uniaxial compressive behavior of closed-cell Al-Si-Ti foams having different relative densities at different strain rates. Special focus was placed upon quantifying the strain rate sensitivity of the material and exploring its underlying mechanisms. Within the range of strain rate considered (0.001 to 2500 s^{-1}), the dynamic deformation of Al-Si-Ti foams having the same relative density was found to be similar to their quasi-static behavior. It was established that the strain rate sensitivity of the foam is derived mainly from that of its parent material, increasing with increasing relative density. It was further established that Al-Si-Ti foams having relatively low relative densities (less than about 0.25) may be approximated as strain-rate insensitive in practical applications, although the critical relative density separating the rate-sensitive and rate-insensitive regimes needs further study especially for other cellular foams made from matrices having different rate dependent properties from the material system studied in this work. Micro-inertia, shock wave, and compressed air pressure in individual cells were found to have negligible effect on the rate sensitivity of the foam, while specimen size (shape) should be carefully selected to minimize specimen size effects.

Funding

This work was supported by the National Basic Research Program of China (2011CB610305), the National Natural Science Foundation of China (11021202), and the Natural Science Foundation of Shaanxi Province (2011JM1012).

References

- [1] J. Banhart, Manufacture, characterisation and application of cellular metals and metal foams, *Prog. Mater. Sci.*, vol. 46, pp. 559–632, 2001.
- [2] I.W. Hall, M. Guden, and C.J. Yu, Crushing of aluminum closed cell foams: Density and strain rate effects, *Scr. Mater.*, vol. 43, pp. 515–521, 2000.
- [3] L. Peroni, M. Avalle, and M. Peroni, The mechanical behaviour of aluminium foam structures in different loading conditions, *Int. J. Impact Eng.*, vol. 35, pp. 644–658, 2008.
- [4] H. Zhao, I. Elnasri, and H. Li, The mechanism of strength enhancement under impact loading of cellular materials, *Adv. Eng. Mater.*, vol. 8, pp. 877–883, 2006.
- [5] T. Mukai, H. Kanahashi, T. Miyoshi, M. Mabuchi, T.G. Nieh, and K. Higashi, Experimental study of energy absorption in a closed-celled aluminum foam under dynamic loading, *Scr. Mater.*, vol. 40, pp. 921–927, 1999.
- [6] K.A. Dannemann and J. Lankford, High strain rate compression of closed-cell aluminium foams, *Mater. Sci. Eng., A*, vol. 293, pp. 157–164, 2000.
- [7] T. Mukai, T. Miyoshi, S. Nakano, H. Somekawa, and K. Higashi, Compressive response of a closed-cell aluminum foam at high strain rate, *Scr. Mater.*, vol. 54, pp. 533–537, 2006.
- [8] C.M. Cady, G.T.I. Gray, C. Liu, M.L. Lovato, T. Mukai, D.P. Mondal, M.D. Goel, and S. Das, Compressive properties of a closed-cell aluminum foam as a function of strain rate and temperature, *Mater. Sci. Eng., A*, vol. 525, pp. 1–6, 2009.
- [9] H. Zhao, I. Elnasri, and S. Abdennadher, An experimental study on the behaviour under impact loading of metallic cellular materials, *Int. J. Mech. Sci.*, vol. 47, pp. 757–774, 2005.
- [10] V.S. Deshpande and N.A. Fleck, High strain rate compressive behaviour of aluminium alloy foams, *Int. J. Impact Eng.*, vol. 24, pp. 277–298, 2000.
- [11] R.E. Raj, V. Parameswaran, and B.S.S. Daniel, Comparison of quasi-static and dynamic compression behavior of closed-cell aluminum foam, *Mater. Sci. Eng., A*, vol. 526, pp. 11–15, 2009.
- [12] S. Yu, Y. Luo, and H. Liu, Effects of strain rate and SiC particle on the compressive property of SiCp/AlSi9Mg composite foams, *Mater. Sci. Eng., A*, vol. 487, pp. 394–399, 2008.
- [13] Z.Y. Dou, L.T. Jiang, G.H. Wu, Q. Zhang, Z.Y. Xiu, and G.Q. Chen, High strain rate compression of cenosphere-pure aluminum syntactic foams, *Scr. Mater.*, vol. 57, pp. 945–948, 2007.
- [14] Y.H. Mu, G.C. Yao, Z.K. Cao, H.J. Luo, and G.Y. Zu, Strain-rate effects on the compressive response of closed-cell copper-coated carbon fiber/aluminum composite foam, *Scr. Mater.*, vol. 64, pp. 61–64, 2011.
- [15] E.W. Andrews, G. Gioux, P. Onck, and L.J. Gibson, Size effects in ductile cellular solids. Part II: Experimental results, *Int. J. Mech. Sci.*, vol. 43, pp. 701–713, 2001.
- [16] D.J. Frew, M.J. Forrestal, and W. Chen, Pulse shaping techniques for testing elastic-plastic materials with a split Hopkinson pressure bar, *Exp. Mech.*, vol. 45, pp. 186–195, 2005.
- [17] Y. Feng, Z.G. Zhu, F.Q. Zu, S.S. Hu, and Y. Pan, Strain rate effects on the compressive property and the energy-absorbing capacity of aluminum alloy foams, *Mater. Charact.*, vol. 47, pp. 417–422, 2001.
- [18] L.L. Wang, *Foundation of Stress Waves*, National Defense Industry Press, Beijing, China, 2005.
- [19] M.J. Silva, W.C. Hayes, and L.J. Gibson, The effects of nonperiodic microstructure on the elastic properties of 2-dimensional cellular solids, *Int. J. Mech. Sci.*, vol. 37, pp. 1161–1177, 1995.
- [20] C. Kádár, E. Maire, A. Borbély, G. Peix, J. Lendvai, and Z. Rajkovits, X-ray tomography and finite element simulation of the indentation behavior of metal foams, *Mater. Sci. Eng., A*, vol. 387, pp. 321–325, 2004.
- [21] G.W. Ma, Z.Q. Ye, and Z.S. Shao, Modeling loading rate effect on crushing stress of metallic cellular materials, *Int. J. Impact Eng.*, vol. 36, pp. 775–782, 2009.
- [22] X.Y. Su, T.X. Yu, and S.R. Reid, Inertia-sensitive impact energy-absorbing structures. 2. Effect of strain-rate, *Int. J. Impact Eng.*, vol. 16, pp. 673–689, 1995.
- [23] A. Paul and U. Ramamurty, Strain rate sensitivity of a closed-cell aluminum foam, *Mater. Sci. Eng., A*, vol. 281, pp. 1–7, 2000.
- [24] A. Tasdemirci, C. Ergonenc, and M. Guden, Split Hopkinson pressure bar multiple reloading and modeling of a 316 L stainless steel metallic hollow sphere structure, *Int. J. Impact Eng.*, vol. 37, pp. 250–259, 2010.
- [25] F.S. Han, H.F. Cheng, Z.B. Li, and Q. Wang, The strain rate effect of an open cell aluminum foam, *Metall. Mater. Trans. A*, vol. 36A, pp. 645–650, 2005.
- [26] T. Mukai, H. Kanahashi, K.S.Y. Yamada, M. Mabuchi, T.G. Nieh, and K. Higashi, Dynamic compressive behavior of an ultralightweight magnesium foam, *Scr. Mater.*, vol. 41, pp. 365–371, 1999.
- [27] C. Park and S.R. Nutt, Strain rate sensitivity and defects in steel foam, *Mater. Sci. Eng., A*, vol. 323, pp. 358–366, 2002.
- [28] Y.D. Liu, J.L. Yu, Z.J. Zheng, and J.R. Li, A numerical study on the rate sensitivity of cellular metals, *Int. J. Solids Struct.*, vol. 46, pp. 3988–3998, 2009.
- [29] L.J. Gibson and M.F. Ashby, *Cellular Solids: Structure and Properties*, 2nd Edition, Cambridge University Press, Cambridge, UK, 1997.
- [30] Z. Zheng, J. Yu, and J. Li, Dynamic crushing of 2D cellular structures: A finite element study, *Int. J. Impact Eng.*, vol. 32, pp. 650–664, 2005.
- [31] G.H. Wu, Z.Y. Dou, D.L. Sun, L.T. Jiang, B.S. Ding, and B.F. He, Compression behaviors of cenosphere-pure aluminum syntactic foams, *Scr. Mater.*, vol. 56, pp. 221–224, 2007.
- [32] W.G. Guo, Y.L. Li, and F.Z. Huang, Deformation and mechanical property of aluminium foam at different strain rates, *Explos. Shock Waves*, vol. 28, pp. 289–292, 2008.
- [33] L. Jing, Z.H. Wang, J.G. Ning, and L.M. Zhao, The dynamic response of sandwich beams with open-cell metal foam cores, *Composites Part B*, vol. 42, pp. 1–10, 2011.
- [34] Y.F. Zhang, Y.Z. Tang, G. Zhou, J.N. Wei, and F.S. Han, Dynamic compression properties of porous aluminum, *Mater. Lett.*, vol. 56, pp. 728–731, 2002.
- [35] A.G. Hanssen, O.S. Hopperstad, M. Langseth, and H. Ilstad, Validation of constitutive models applicable to aluminium foams, *Int. J. Mech. Sci.*, vol. 44, pp. 359–406, 2002.